No. 68-67

THE HYPERSONIC LAMINAR BOUNDARY LAYER APPROACHING THE BASE OF A SLENDER BODY

by

G. R. OLSSON and A. F. MESSITER
The University of Michigan
Ann Arbor, Michigan

AIAA Paper
No. 68-67

AIAA 6th Aerospace Sciences Meeting

NEW YORK, NEW YORK / JANUARY 22-24, 1968

THE HYPERSONIC LAMINAR BOUNDARY LAYER APPROACHING THE BASE OF A SLENDER BODY

G. R. Olsson* and A. F. Messiter†
The University of Michigan, Ann Arbor, Michigan

An asymptotic description is obtained for the acceleration of a laminar hypersonic boundary layer approaching a sharp corner, assuming small interaction with the outer inviscid flow. Viscous forces are neglected except in a thin sublayer. The initial part of the expansion takes place over a distance $O(M_e\bar{\delta})$, where M_e is the external Mach number and $\bar{\delta}$ is the boundary-layer thickness. Here the transverse pressure gradient is small and a solution can be obtained analytically. Within a distance $O(\bar{\delta})$ from the corner, the effect of streamline curvature is essential, and a numerical solution is obtained by the method of integral relations for a single strip. The solution for surface pressure is compared with experimental results for a particular case, and an approximate velocity profile at the corner is calculated. Possibilities for improving the accuracy are considered, both by refining the numerical procedure and by including higher-order effects.

SYMBOLS

A	Constant defined in Eq. (42)
$a_m(\xi)$, $b_m(\xi)$	Coefficients in representations of Θ and Θ^{-1}, Eq. (53)
$c_0(\tilde{x})$, $c_1(\tilde{x})$	Coefficients in representation of $\tilde{\rho}\tilde{u}$, Eq. (40)
$d_0(\tilde{x})$, $d_1(\tilde{x})$	Coefficients in representation of $\tilde{\rho}\tilde{u}\tilde{v}$, Eq. (44)
E	Function defined in Eq. (10)
f_k	Weighting functions in method of integral relations
g	Transformed stream function, defined preceding Eq. (9)
j	0, 1 for wedge or cone respectively
k	Index defining strip boundary for method of integral relations calculation
L	Length of body
M	Mach number
N	Number of strips in method of integral relations calculation
p	Pressure
R_w	Reynolds number based on free-stream velocity, body length, and thermodynamic properties at the body surface
s	Streamwise coordinate, equal to $\hat{x}$
T	Temperature
U	Nondimensional velocity at outer edge of sublayer
u, v	Velocity components in x, y directions respectively
w	Transformed normal velocity component defined following Eq. (52)
x, y	Coordinates measured along and normal to body surface respectively
α	Constant $g''(0) = 0.4696$
β	Similarity variable, related to stream function by Eq. (9)
γ	Ratio of specific heats
δ	Boundary-layer thickness, taken equal to δ^*
δ^*	Displacement thickness
η	Transformed normal coordinate, Eq. (50)
Θ	$(\partial u^\dagger/\partial \eta)^{-1}$
θ	Flow deflection angle
μ	Viscosity coefficient
ξ	Transformed streamwise coordinate, Eq. (50)
ρ	Density
τ	Wedge or cone half-angle
ϕ	Transformed streamwise coordinate, Eq. (30)
ψ	Stream function

Subscripts

c	Denotes value corresponding to critical profile
e	Denotes value at outer edge of undisturbed boundary layer
w	Denotes value at body surface in undisturbed boundary layer
δ	Denotes value at outer edge of accelerating boundary layer
o	Denotes value for $\tilde{y} \to 0$
1	Denotes value for undisturbed boundary layer at $\bar{x} = L$

Superscripts

–	Denotes dimensional quantity
^	Denotes nondimensional function of $\hat{x} = (\bar{x} - L)/M_e R_w^{-\frac{1}{2}} L$ and $\tilde{y} = \bar{y}/R_w^{-\frac{1}{2}} L$, Eq. (4)

This work was supported by the Advanced Research Projects Agency under Contract DAHC15 67 C 0062, as a part of Project DEFENDER.

*Graduate student, Department of Aerospace Engineering; now Project Scientist, Booz-Allen Applied Research, Inc., Bethesda, Md. Member AIAA.

†Associate Professor of Aerospace Engineering. Member AIAA.

Denotes nondimensional function
$\tilde{x} = (\bar{x} - L)/R_w^{-1/2} L$ and
$\tilde{y} = \bar{y}/R_w^{-1/2} L$, Eq. (15)

† Denotes nondimensional function of
$\tilde{x} = (\bar{x} - L)/R_w^{-1/2} L$ and
$y^\dagger = \bar{y}/R_w^{-3/4} L$, Eq. (25)

1. INTRODUCTION

Calculation of the flow in the near wake of a slender body at hypersonic speed requires detailed knowledge of the boundary-layer expansion and separation in the neighborhood of the sharp corner at the base. Measurements by Hama[1] have emphasized the complicated nature of the flow immediately downstream of the corner. His data also show the expected result that a significant fraction of the pressure drop occurs upstream of the corner. The present investigation is concerned with the details of this part of the flow just upstream of the corner, for the case of a thin laminar boundary layer along a slender wedge or cone at high Mach number. For simplicity, zero wall heat transfer is assumed, and the gas is considered to be perfect and nonreacting, with constant specific heats, viscosity proportional to temperature, and Prandtl number equal to one.

Since the Mach number is large, the temperature in the boundary layer is high, the density and mass flow are small, and the boundary-layer thickness, δ, is taken equal to the displacement thickness $\bar{\delta}^*$ (see, for example, Moore[2]). The Mach number M_e outside the boundary layer is of order $1/\tau$, where τ is the wedge or cone half-angle. Also, $\bar{\delta}^*/L = O(R_w^{-1/2})$, where L is the body length and R_w is the Reynolds number based on the free-stream velocity, the body length, and the density and viscosity evaluated at the wall. Then the boundary-layer thickness is small compared with the distance from the body surface to the shock wave, provided that the interaction parameter $M_e R_w^{-1/2}$ is small.

Near the corner the flow outside the boundary layer may be approximated as a centered Prandtl-Meyer expansion. The expansion actually begins somewhat ahead of the corner, because disturbances can propagate upstream through the subsonic part of the layer. For a fluid element inside the boundary layer, pressure and inertia forces rapidly grow larger as the element approaches the corner, while viscous forces remain of the same order as further upstream, except in a thin sublayer. Outside this sublayer, therefore, the accelerating boundary-layer flow may be described approximately by inviscid-flow equations. Since the base pressure is known from experiment[1] to be sufficiently low, a fluid element initially at the surface (i.e., just outside the thin sublayer) will accelerate at least to sonic speed at the corner. The sonic line is not expected to intersect the surface upstream of the corner, because streamlines near the surface would have to bend away from the wall as the pressure continues to decrease. In this approximation, therefore, the sonic line is required to terminate at the corner, and the flow upstream of the corner can be studied without further knowledge of the downstream flow. A sketch of the flow details is shown in Fig. 1.

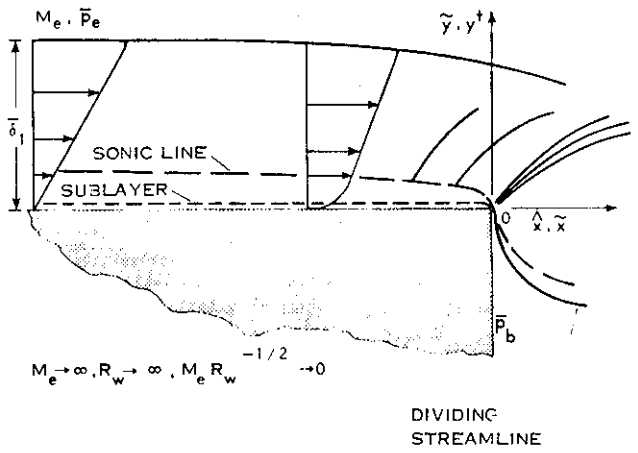

Figure 1. Acceleration of a Hypersonic Boundary Layer Approaching a Corner

The idea of describing abrupt changes in a boundary layer by the inviscid-flow equations appears in the literature in several different contexts. For example, Morkovin[3] has observed experimentally the effect of an expansion wave impinging upon a boundary layer on the wall of a supersonic wind tunnel, and finds that an inviscid-flow calculation successfully predicts the post-interaction velocity profile except in a thin sublayer. Lighthill[4] analyzes the interaction of a supersonic boundary layer with a weak pressure disturbance by introducing small perturbations on a parallel shear flow and neglecting viscous forces except in a sublayer. Zakkay and Tani[5] use the concept of a sublayer in studing the boundary layer just downstream of a sharp corner, as at the shoulder of a cone-cylinder, with the initial profile obtained by assuming an inviscid expansion at the corner. For the same case, an approximate calculation of changes close to the corner is given by Hunt and Sibulkin,[6] using a momentum integral and assuming pressure constant along radial lines.

A numerical solution of the problem to be discussed here has been obtained by Baum,[7] using a finite-difference method to solve the boundary-layer equations, supplemented for the initially supersonic portion of the flow by an inviscid transverse momentum equation; the normal pressure gradient is zero for the initially subsonic part. Weiss and Nelson[8] have obtained an approximate solution by using a stream-tube calculation (zero normal pressure gradient) for the fluid which is initially at subsonic speed and a Prandtl-Meyer expansion for the initially supersonic part. In the present investigation, approximate equations are derived which are expected to be correct in an asymptotic sense for the case of a sufficiently thin hypersonic boundary layer, a method is shown for obtaining approximate numerical results, and the procedures for studying the largest neglected terms are considered.

In the present approach, use of the hypersonic approximation leads to two distinct inviscid-flow problems. If the relative pressure change is of order one, the flow deflection θ_δ at the outer edge of the boundary layer is of order $1/M_e$. If the flow deflection θ is also $O(1/M_e)$ inside the layer, the streamline curvature is small and the normal pressure gradient is approximately zero. But if $\theta = O(1)$ inside the layer, the streamline curvature and the normal pressure gradient can no longer be neglected. Thus two different descriptions, and two different sets of approximate equations, might be anticipated. It would appear that both kinds of behavior really do occur. As the pressure $\bar{p}$ first begins to decrease, changes in streamtube area in the subsonic portion of the layer are dominant. The boundary layer gradually becomes thinner, and $\theta = O(1/M_e)$ throughout the layer. Here the boundary layer may be called subcritical (see, e.g., the discussion by Lees and Reeves[9]). But as the flow continues to accelerate, a critical value $\bar{p}_c$ of the pressure is reached. For a further pressure decrease, the spreading of streamlines in the supersonic region will dominate. This can take place only very close to the corner, where the flow becomes free to turn inward. Since the base pressure is known from experiment to be quite low, this further pressure drop is required, and it will be necessary that $\theta = O(1)$ in order that a sufficient pressure decrease may occur.

The approximations outlined in the preceding paragraph are expected to describe the asymptotic behavior of the flow in the case of a thin laminar boundary layer at high Mach number. The hypersonic boundary-layer approximation corresponds to the limit $M_e \to \infty$, $R_w \to \infty$, and $M_e R_w^{-1/2} \to 0$, with $\bar{x}/L$ and $\bar{y}/R_w^{-1/2}L$ head fixed, where $\bar{x}$ and $\bar{y}$ are coordinates measured, respectively, along and normal to the body surface, with the vertex as origin. The two types of behavior discussed in the preceding paragraph are obtained by taking limits with $(\bar{x}/L - 1)/M_e R_w^{-1/2}$ and $(x/L - 1)/R_w^{-1/2}$ fixed. An important feature of the approximation is that the value of M_e need not be specified until the end of the calculation, when solutions in the two limits are combined for a particular case. The motivation for the choices of stretched coordinates, and for the choice of a limit process to describe the sublayer, is discussed in Section 2.

In Section 3 it is shown that solutions to the corresponding approximate equations can actually be obtained, and satisfy all the necessary boundary and matching conditions. The existence of these solutions provides a strong further justification for the approximation procedure used. The approximate equations obtained in the first limit can be integrated directly, and the solution is found to break down when the pressure reaches a value such that

$$\int_0^{\bar{\delta}} (M^{-2} - 1)\, d\bar{y} = 0 \qquad (1)$$

where M is the local Mach number. This integral appears in Lighthill's[4] work, and its importance has also been noted by Lees.[10] The approximate equations obtained in the second limit are solved by the method of integral relations for a single strip, and the sublayer equations are studied in a similar way. In Section 4 the predicted surface pressure is compared with experiment[1] for a particular case, and an approximate velocity profile at the corner is calculated. Possibilities for improvement are considered, both by refining the numerical procedure and by including higher-order effects.

2. ASYMPTOTIC REPRESENTATIONS

A decrease in pressure initially causes the boundary layer on the wedge or cone to become thinner, and it is expected that the corresponding flow deflection is $O(1/M_e)$ throughout the layer as well as at the outer edge. The thickness $\bar{\delta}^*$ continues to decrease until a critical value of the pressure $\bar{p}$ is reached such that $d\bar{\delta}^*/d\bar{p} = 0$. Since small changes in the initial profile would not be sufficient to bring about this condition, along a streamline the required relative changes in pressure, density, and velocity will be of order one. Since the approximate continuity equation must show a balance between streamline divergence and change in mass flux, it follows that the initial part of the expansion takes place over a distance $\Delta\bar{x} = O(M_e R_w^{-1/2} L)$ upstream from the corner. The ratio of this distance to the body length is of the same order as the ratio of the boundary-layer thickness to the distance between the body surface and the shock wave. The present work is concerned only with values of the parameters such that $M_e R_w^{-1/2}$ is small.

Thus it is appropriate to introduce stretched coordinates

$$\hat{\bar{x}} = (\bar{x} - L)/M_e R_w^{-\frac{1}{2}} L\,, \quad \hat{\bar{y}} = \bar{y}/R_w^{-\frac{1}{2}} L \qquad (2)$$

and to study a limit

$$M_e \to \infty\,,\ R_w \to \infty\,,\ M_e R_w^{-\frac{1}{2}} \to 0 \qquad \hat{\bar{x}},\ \hat{\bar{y}} \text{ fixed} \qquad (3)$$

Since $\Delta\bar{p}/\bar{p} = O(1)$, $\bar{T}/\bar{T}_e = O(M_e^2)$, and $\theta = O(1/M_e)$, the asymptotic representations in this limit are expected to be of the form

$$\bar{u}/\bar{u}_e \sim \hat{\bar{u}}(\hat{\bar{x}}, \hat{\bar{y}}) + \cdots\,, \quad \bar{p}/\bar{\rho}_w \bar{u}_e^2 \sim \hat{\bar{p}}(\hat{\bar{x}}, \hat{\bar{y}}) + \cdots$$
$$\bar{v}/\bar{u}_e \sim M_e^{-1} \hat{\bar{v}}(\hat{\bar{x}}, \hat{\bar{y}}) + \cdots\,, \quad \bar{\rho}/\bar{\rho}_w \sim \hat{\bar{\rho}}(\hat{\bar{x}}, \hat{\bar{y}}) + \cdots \qquad (4)$$

where $\bar{u}$, $\bar{v}$ are the velocity components in the $\bar{x}$, $\bar{y}$ directions, respectively; $\bar{p}, \bar{\rho}$ and $\bar{T}$ are the pressure, density, and temperature; and the subscripts w, e denote conditions in the undisturbed boundary layer, at the wall and at the outer edge, respectively.

The approximate equations to be satisfied by the functions $\hat{u}$, $\hat{v}$, $\hat{p}$, and $\hat{\rho}$ are obtained from the full Navier-Stokes equations by taking the limit (3), and are most conveniently expressed in terms of von Mises coordinates $s, \hat{\psi}$ defined by

$$s = \hat{x} \quad , \quad \hat{\psi}_{\tilde{y}} = \hat{\rho}\hat{u}, \quad \hat{\psi}_{\hat{x}} = -\hat{\rho}\hat{v} \tag{5}$$

Since the upstream influence of the corner is small, the flow is nearly two-dimensional both for the wedge and for the cone. The approximate continuity and normal momentum equations are

$$(\hat{v}/\hat{u})_{\hat{\psi}} = (1/\hat{\rho}\hat{u})_{s} \quad , \quad \hat{p}_{\hat{\psi}} = 0 \tag{6}$$

where $\hat{u}$, $\hat{v}$, $\hat{p}$, and $\hat{\rho}$ are now to be regarded as functions of s and $\hat{\psi}$. The entropy of a fluid element is approximately constant, and, because the wall heat transfer is zero and the Prandtl number equals one, the total enthalpy is uniform:

$$\hat{p} = E(\hat{\psi})\,\hat{\rho}^{\gamma} \quad , \quad \hat{u}^2 + [2\gamma/(\gamma-1)]\,\hat{p}/\hat{\rho} = 1 \tag{7}$$

where $E(\hat{\psi})$ will be expressed in terms of the initial velocity profile. The approximation $M_e >> 1$ has been used to evaluate the total enthalpy. Equations (6) and (7) are inviscid-flow equations with zero normal pressure gradient; essentially the same equations were described as "inviscid boundary-layer equations" in a study by Cole and Aroesty [1] of boundary layers with strong blowing. The largest neglected terms in Eqs. (6) and (7) are $O(M_e R_w^{-1/2})$ and $O(M_e^{-2})$.

Initially the velocity profile is the boundary-layer profile for a wedge or cone, evaluated at $\bar{x} = L$:

$$\hat{u}(-\infty, \hat{\psi}) = g'(\beta) \tag{8}$$

Here β is defined by

$$\beta = \left(2\int_0^x r^{2j}\,dx\right)^{-\frac{1}{2}} r^j \int_0^{\tilde{y}} (\bar{\rho}/\bar{\rho}_w)\,d\tilde{y}$$

where $x = \bar{x}/L$ and $r = x$; $j = 0$ for a wedge and $j = 1$ for a cone. The function $g(\beta)$ is the Blasius solution, satisfying $g''' + g\,g'' = 0$, $g(0) = g'(0) = 0$, and $g'(\infty) = 1$. At $x = 1$,

$$d\hat{\psi} = [2/(2j+1)]^{\frac{1}{2}}\, g'(\beta)\, d\beta \tag{9}$$

Thus β = constant along $\hat{\psi}$ = constant, and each value of β identifies a streamline. Since $\hat{\rho}(-\infty, 0) = 1$ and $\bar{p}_e/\bar{p}_w\bar{u}_e^2 = (\gamma-1)/2\gamma$, $E(\hat{\psi})$ is given by

$$E(\hat{\psi}) = [(\gamma-1)/2\gamma]\,(1 - g'^2)^{\gamma} \tag{10}$$

At the wall the boundary condition to be imposed is

$$\hat{v}(s, 0) = 0 \tag{11}$$

and the no-slip condition must be dropped because viscous effects do not appear in the approximate equations. At the outer edge of the boundary layer the pressure and flow deflection are related by the hypersonic small-disturbance approximation for a simple wave (given, e.g., by Liepmann and Roshko [2]). Since $\hat{p} = \hat{p}(s)$,

$$\hat{p}(s) = [(\gamma-1)/2\gamma]\,[1 + \tfrac{1}{2}(\gamma-1)\,\hat{v}(s,\infty)]^{2\gamma/(\gamma-1)} \tag{12}$$

As the pressure continues to decrease, the spreading of streamlines in the supersonic portion of the boundary layer become dominant. Since the base pressure is sufficiently low, the further relative changes in pressure, density, and velocity must be of order one. Relative changes in streamtube area must also be of order one. Because the outer edge of the layer is effectively constrained, the change in streamtube area can only occur if $\theta = O(1)$ for a distance $O(R_w^{-1/2} L)$ upstream from the corner. The same conclusion would be reached by studying the equations in a more formal way. It will be evident from the solutions that the system (6), (7), (8), (11), and (12) is not capable of describing the flow all the way to the corner. If new approximate equations are really to describe a different type of behavior, it is necessary that the effect of streamline curvature be retained. It is assumed that $\bar{p}$, $\bar{\rho}$, and $\bar{u}$ undergo relative changes of order one, and the order estimates for θ and $\bar{x} - L$ are obtained by requiring the appropriate balance of terms in the $\bar{y}$-momentum equation and in the continuity equation. Further justification for these ideas is provided by the result (in Section 3) that solutions can actually be obtained satisfying all the prescribed conditions.

Thus the critical point, where $d\bar{\delta}^*/d\bar{p}$ becomes zero, is located at a distance $o(M_e R_w^{-1/2} L)$ from the corner, i.e., at $\hat{x} = 0$, and the remaining part of the upstream expansion should be described in terms of coordinates

$$\tilde{X} = (\bar{x} - L)/R_w^{-\frac{1}{2}} L \quad , \quad \tilde{y} = \bar{y}/R_w^{-\frac{1}{2}} L \tag{13}$$

The appropriate limit is

$$M_e \to \infty \ , \ R_w \to \infty \ , \ M_e R_w^{-\frac{1}{2}} \to 0 \qquad \tilde{x},\ \tilde{y} \text{ fixed} \tag{14}$$

The boundary-layer thickness will be expressed by $\delta = \bar{\delta}/R_w^{-1/2}L$, and is approximately constant in the limit (14) because $d\bar{\delta}^*/d\bar{x} \approx \theta_\delta << 1$ for $M_e >> 1$

The assumed asymptotic representations are

$$\bar{u}/\bar{u}_e \sim \tilde{u}(\tilde{x}, \tilde{y}) + \cdots, \quad \bar{p}/\bar{\rho}_w \bar{u}_e^2 \sim \tilde{p}(\tilde{x}, \tilde{y}) + \cdots$$
$$\bar{v}/\bar{u}_e \sim \tilde{v}(\tilde{x}, \tilde{y}) + \cdots, \quad \bar{\rho}/\bar{\rho}_w \sim \tilde{\rho}(\tilde{x}, \tilde{y}) + \cdots \tag{15}$$

The approximate equations to be satisfied by these functions are obtained from the full Navier-Stokes equations by taking the limit (14). A convenient form is

$$(\tilde{\rho}\tilde{u})_{\tilde{x}} + (\tilde{\rho}\tilde{v})_{\tilde{y}} = 0, \quad (\tilde{\rho}\tilde{u}\tilde{v})_{\tilde{x}} + (\tilde{p} + \tilde{\rho}\tilde{v}^2)_{\tilde{y}} = 0 \tag{16}$$

$$\tilde{u}^2 + \tilde{v}^2 + [2\gamma/(\gamma - 1)]\,\tilde{p}/\tilde{\rho} = 1, \quad \tilde{p} = E\tilde{\rho}^\gamma \tag{17}$$

where E is again given by Eq. (10). At the body surface it is required that

$$\tilde{v}(\tilde{x}, 0) = 0 \tag{18}$$

and the no-slip condition is again lost. At the outer edge $\tilde{y} = \delta$, the flow deflection is small, so that in the first approximation it is required that

$$\tilde{v}(\tilde{x}, \delta) = 0 \tag{19}$$

It will also be necessary to require that $\tilde{p}(\tilde{x}, \delta)$ be bounded and nonzero. To obtain initial conditions upstream it is assumed that for any given flow quantity the solution obtained in the limit (3) for $\hat{x}$ fixed can be matched asymptotically with the solution obtained in the limit (14) for $\tilde{x}$ fixed. That is, it is assumed that both solutions are valid approximations for some class of intermediate limits such that

$$\tilde{x} \to -\infty, \quad \tilde{x}/M_e \to 0, \quad \tilde{x}/f(M_e) \text{ fixed} \tag{20}$$

where $1 << f(M_e) << M_e$ for $M_e >> 1$ (Kaplum[13]).
In the first approximation the matching appears straightforward, and the matching conditions to be used are simply.

$$\tilde{u}(-\infty, \tilde{y}) = \hat{u}(0, \tilde{y}), \quad \tilde{p}(-\infty, \tilde{y}) = \hat{p}(0), \quad \tilde{v}(-\infty, \tilde{y}) = 0 \tag{21}$$

where $\hat{u}$ and $\hat{p}$ are defined by Eq. (4), and the result $\hat{p} = \hat{p}(\hat{x})$ has been used.

Since it is assumed that a common region of validity exists for the solutions obtained in the two limits (3) and (14), composite solutions may be formed which are uniformly valid approximations in the region of interest $-\infty < \hat{x} \le 0$. For each flow quantity the composite expansion is formed by adding the two solutions and subtracting the common part:

$$\bar{u}/\bar{u}_e \sim \hat{u}(\hat{x}, \tilde{y}) + \tilde{u}(\tilde{x}, \tilde{y}) - \hat{u}(0, \tilde{y})$$
$$\bar{p}/\bar{p}_e \sim \hat{p}(\hat{x}) + \tilde{p}(\tilde{x}, \tilde{y}) - \hat{p}(0) \tag{22}$$
$$\bar{v}/\bar{u}_e \sim \tilde{v}(\tilde{x}, \tilde{y})$$

In the limit for $\hat{x}$ fixed, $\bar{v}/\bar{u}_e$ is small, and so the solution obtained for $\tilde{x}$ fixed is already uniformly valid to order one.

Since the no-slip condition is violated by solutions to the approximate equations given above, a thin viscous sublayer must exist in which viscous, pressure, and inertia forces are all of the same order of magnitude. If the sublayer were studied in the hypersonic limit $M_e \to \infty$, it would be necessary to consider one sublayer solution for $\hat{x}$ fixed and another for $\tilde{x}$ fixed. In a first approximation it is doubtful that anything is gained by this increased complication. Therefore the procedure chosen is to consider a limit $R_w \to \infty$ with M_e fixed. This means that the matching conditions for $\bar{u}$ and $\bar{p}$ at the outer edge of the sublayer are expressed in terms of the composite expansions given in Eq. (22), and the $\bar{x}$ coordinate is stretched by a factor $R_w^{-1/2}L$. It is now necessary to specify M_e, because $\hat{x}$ is to be replaced by $M_e^{-1}\tilde{x}$, but a value of R_w still is not required. As in ordinary boundary-layer theory, an order estimate for the sublayer thickness, which will be a proper stretching factor for the $\bar{y}$ coordinate, is found by requiring a balance between inertia and viscous forces in the momentum equation. This estimate is $O(R_w^{-3/4}L)$, and so it is appropriate to introduce a stretched $\bar{y}$ coordinate.

$$y^\dagger = \bar{y}/R_w^{-\frac{3}{4}}L \tag{23}$$

The limit to be considered is therefore

$$R_w \to \infty; \quad \tilde{x}, y^\dagger, M_e \text{ fixed} \tag{24}$$

The asymptotic representations are

$$\bar{u}/\bar{u}_e \sim U(\tilde{x})\,u^\dagger(\tilde{x}, y^\dagger) + \cdots$$
$$\bar{v}/\bar{u}_e \sim R_w^{-\frac{1}{4}}\,U(\tilde{x})\,v^\dagger(\tilde{x}, y^\dagger) + \cdots$$
$$\bar{p}/\bar{\rho}_w \bar{u}_e^2 \sim p^\dagger(\tilde{x}) + \cdots \tag{25}$$
$$\bar{\rho}/\bar{\rho}_w \sim \rho^\dagger(\tilde{x}, y^\dagger) + \cdots$$

where $U(\tilde{x})$ is the expression for $\bar{u}/\bar{u}_e$ obtained from the composite solution (22) by setting $\tilde{y} = 0$, and $p^\dagger$ has been written as $p^\dagger(\tilde{x})$ in anticipation of the approximate $\bar{y}$-momentum equation $p^\dagger_{y^\dagger} = 0$.
The approximate continuity, $\bar{x}$-momentum and energy equations are

$$(\rho^\dagger U u^\dagger)_{\tilde{x}} + (\rho^\dagger U v^\dagger)_{y^\dagger} = 0 \tag{26}$$

$$\rho^\dagger U u^\dagger (U u^\dagger)_{\tilde{x}} + \rho^\dagger U^2 v^\dagger u^\dagger{}_{y^\dagger} = -dp^\dagger/d\tilde{x} + U(\mu^\dagger u^\dagger{}_{y^\dagger})_{y^\dagger} \tag{27}$$

$$U^2 u^{\dagger 2} + [2\gamma/(\gamma - 1)]\, p^\dagger/\rho^\dagger = 1 \qquad (28)$$

The viscosity $\mu^\dagger = \bar{\mu}/\bar{\mu}_w$ will be assumed linear in $\bar{T}/\bar{T}_w$. The boundary and matching conditions are

$$u^\dagger(\tilde{x}, 0) = v^\dagger(\tilde{x}, 0) = 0 \quad , \quad u^\dagger(\tilde{x}, \infty) = 1 \qquad (29)$$

and the pressure $p^\dagger(\tilde{x})$ is found from the composite expansion (22) for $\bar{p}$, evaluated at $\tilde{y} = 0$. A condition on the behavior of the sublayer solution for $\tilde{x} \to -\infty$ will be given later.

3. SOLUTIONS

The solutions to Eqs. (6) and (7), subject to the boundary and initial conditions (8), (11), and (12), are conveniently expressed in terms of a transformed $\tilde{x}$-coordinate defined by

$$\phi = 1 + \tfrac{1}{2}(\gamma - 1)\,\hat{v}(s, \infty) \qquad (30)$$

where the function $\hat{v}(s, \infty)$ is to be determined. Solutions in terms of ϕ are found to be

$$\hat{p} = [(\gamma - 1)/2\gamma]\,\phi^{2\gamma/(\gamma - 1)} \qquad (31)$$

$$\hat{\rho} = (1 - g'^2)^{-1}\,\phi^{2/(\gamma - 1)} \qquad (32)$$

$$\hat{u} = [1 - \phi^2(1 - g'^2)]^{\frac{1}{2}} \qquad (33)$$

$$\hat{v} = \hat{u}(ds/d\phi)^{-1} \int_0^{\hat{\psi}} (1/\hat{\rho}\hat{u})_\phi \, d\hat{\psi} \qquad (34)$$

By the definition (30) of ϕ, $\hat{v} \sim -2(1 - \phi)/(\gamma - 1)$ as $\hat{\psi} \to \infty$. The transformation equation relating s and ϕ is then obtained by letting $\hat{\psi} \to \infty$ in Eq. (34):

$$ds/d\phi = -\tfrac{1}{2}(\gamma - 1)(1 - \phi)^{-1} \int_0^{\infty} (1/\hat{\rho}\hat{u})_\phi \, d\hat{\psi} \qquad (35)$$

For a given value of ϕ, the integrand is a known function of $\hat{\psi}$, and the integration over $\hat{\psi}$ can be carried out numerically. Thus the right-hand side may be regarded as known for each value of ϕ, and integration over ϕ can also be carried out. Numerical results for $\hat{p}$, δ, M_o, and $\hat{u}_o$, where the subscript 0 denotes values at $\tilde{y} = 0$, are plotted in Fig. 2.

It is of interest to note the asymptotic behavior for $s \to -\infty$. Since $g'(\beta) \sim \alpha\beta$ as $\beta \to 0$ (Rosenhead[14]), where $\alpha = 0.4696$, it follows that $\hat{u} \sim (1 - \phi^2 + \alpha^2\beta^2\phi^2)^{\frac{1}{2}}$ as $\beta \to 0$. Also $d\hat{\psi} \sim [2/(2j + 1)]^{\frac{1}{2}}\alpha\beta \, d\beta$ as $\beta \to 0$, and so the largest term for $\phi \to 1$ in the integral in Eq. (35) is $O\{(1 - \phi)^{-\frac{1}{2}}\}$, provided that $\phi < 1$ for $|s| < \infty$ (accelerating flow). It is then found that $\phi \sim 1 - (\gamma - 1)^2\alpha^2(2j + 1)^{-1}s^{-2}$ as $s \to -\infty$.

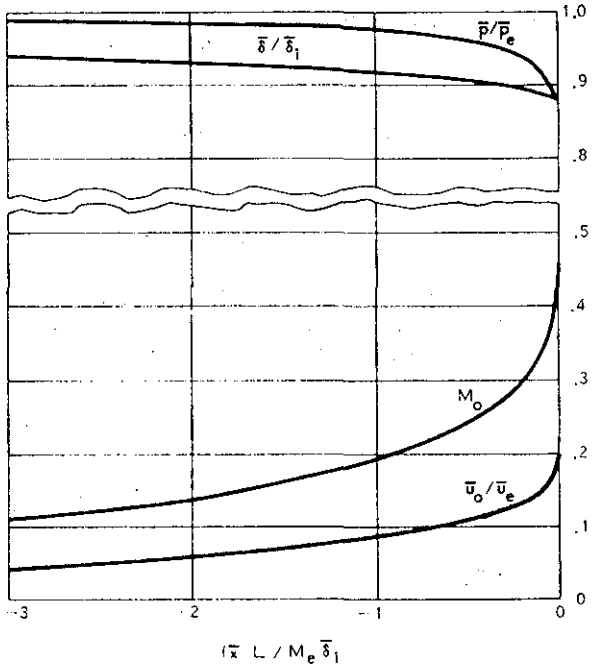

Figure 2. Solution for M_o, $\bar{u}_o/\bar{u}_e$, $\bar{p}/\bar{p}_e$, and $\bar{\delta}/\bar{\delta}_1$

Using Eqs. (32) and (33), together with the definition of the local Mach number M, one can rewrite Eq. (35):

$$ds/d\phi = \phi^{-1}(1 - \phi)^{-1} \int_0^{\delta} (1 - M^{-2})\, d\tilde{y}$$

where $\delta = \bar{\delta}/R_w^{-\frac{1}{2}}L$. As the boundary layer accelerates, a value $\phi = \phi_c$ is reached at which this integral equals zero, and the solution cannot be carried further. This is the critical point, and the constant of integration is chosen such that $s = 0$ there. The critical value of ϕ is found to be $\phi_c = 0.9805$, not much different from one, but the corresponding values of pressure and, especially, Mach number at the wall do show significant change:

$$\bar{p}_c/\bar{p}_e = 0.871 \qquad M_{o,c} = 0.448 \qquad (36)$$

where $\bar{p}_c/\bar{p}_e$ is the ratio of the critical pressure to the pressure in the undisturbed boundary layer, and $M_{o,c}$ is the Mach number at $\tilde{y} = 0$ for the critical profile. The boundary-layer thickness has been reduced by a factor 0.885. The manner in which the flow quantities change as $\phi \to \phi_c$ can be seen if the right-hand side of Eq. (35) is expanded for small $|\phi - \phi_c|$. One finds $ds/d\phi = O(\phi - \phi_c)$, and therefore $s = O[(\phi - \phi_c)^2]$ as $\phi \to \phi_c$. Then, for $\hat{\psi} \to \infty$ and $s \to 0$, $\theta_\delta - \theta_{\delta,c} = O(M_e^{-1}|s|^{\frac{1}{2}})$, while for $s \to 0$ with $\hat{\psi}$ fixed, Eq. (34) gives $\theta = O(M_e^{-1}|s|^{-\frac{1}{2}})$.

That is, the flow deflection inside the boundary layer becomes large compared with M_e^{-1} as $s \to 0$. Also, from Eq. (31), $\bar{p}_c/\bar{p}_e - 1 = O(|s|^{1/2})$ as $s \to 0$.

The solution to Eqs. (16) and (17), subject to the boundary and initial conditions (18), (19), and (21), has been carried out approximately by the method of integral relations (see, for example, Belotserkovskii and Chushkin [15]) for a single strip $0 \le \tilde{y} \le \delta_c$. A formulation for an arbitrary number of strips has also been attempted; this is discussed briefly in Section 4 and in detail by Olsson and Messiter.[16]

For an N-strip calculation the continuity and momentum equation are first integrated across each of the N strips:

$$\int_{y_{k-1}}^{y_k} (\tilde{\rho}\tilde{u})_{\tilde{x}}\, d\tilde{y} = \rho_{k-1} v_{k-1} - \rho_k v_k \qquad (37)$$

$$\int_{y_{k-1}}^{y_k} (\tilde{\rho}\tilde{u}\tilde{v})_{\tilde{x}}\, d\tilde{y} = p_{k-1} + \rho_{k-1} v_{k-1}^2 - p_k - \rho_k v_k^2 \qquad (38)$$

where in general $\delta = \delta(\tilde{x})$; $y_k = k\delta/N$, $k = 1, 2, \ldots, N$; and $p_0 = \tilde{p}(\tilde{x}, 0)$, $p_k = \tilde{p}(\tilde{x}, k\delta/N)$, etc. Each of the functions $\tilde{\rho}\tilde{u}$ and $\tilde{\rho}\tilde{u}\tilde{v}$ is then represented through some simple dependence on $\tilde{y}$, such that the integrations over $\tilde{y}$ can be carried out easily, and N + 1 unknown functions of $\tilde{x}$ are introduced in each of the representations. For example, a suitable representation might be a polynomial of degree N with functions of $\tilde{x}$ as coefficients. In general these representations may be evaluated at each strip boundary in order to relate the new functions of $\tilde{x}$ to the values of the flow quantities there. Additional relations are provided by the entropy and total enthalpy equations evaluated at the strip boundaries, and by the boundary conditions at $\tilde{y} = 0$ and $\tilde{y} = \delta$. The resulting system of equations can be regarded as a system of first-order ordinary differential equations in $\tilde{x}$ for the flow variables at each of the strip boundaries.

A polynomial representation clearly will not be a suitable representation for $\tilde{\rho}\tilde{u}$ because in the hypersonic approximation $\tilde{\rho} \to \infty$ as $\tilde{y} \to \delta$. As $\tilde{y} \to \delta$, or $\beta \to \infty$, the profile $g'(\beta)$ has the behavior[14] $g'(\beta) \sim 1 - 0.331\,(\zeta^{-1} + \ldots) \exp(-\tfrac{1}{2}\zeta^2)$, where $\zeta = \beta - 1.21678$. From Eqs. (32) and (33) it is seen that $1/\hat{\rho} = O(1 - \hat{u})$ as $\hat{u} \to 1$. Using the known behavior of $g'(\beta)$, the expression (9) relating β and $\hat{\psi}$, the definition (5) of $\hat{\psi}$, and the solution (33) for $\hat{u}$, one finds

$$1 - \tilde{y}/\delta = O\left\{(1 - \hat{u})\,[-\log(1 - \hat{u})]^{\frac{1}{2}}\right\} \qquad (39)$$

as $\hat{u} \to 1$ with $\hat{x}$ fixed. These results suggest the correct initial behavior for $\tilde{\rho}\tilde{u}$ as $\tilde{u} \to 1$. As in other applications of the method of integral relations to boundary-layer problems (see, for example, Ref. 15), this behavior is approximated by omitting the logarithmic factor above. Therefore, as $\tilde{y} \to \delta$, $\tilde{\rho}\tilde{u}$ is assumed to be $O\{(1 - \tilde{y}/\delta_c)^{-1}\}$ initially, and the representation to be chosen has this behavior for all $\tilde{x}$. For a one-strip calculation the choice is

$$\tilde{\rho}\tilde{u} = (1 - \tilde{y}/\delta_c)^{-1}\,[c_0(\tilde{x}) + c_1(\tilde{x})\,\tilde{y}/\delta_c] \qquad (40)$$

It is convenient also to introduce the notation $A = c_0(\tilde{x}) + c_1(\tilde{x})$. Using the representation (40) for $\tilde{\rho}\tilde{u}$, one finds that the stream function $\tilde{\psi}$ is expressed by

$$\tilde{\psi} = \int_0^{\tilde{y}} \tilde{\rho}\tilde{u}\, d\tilde{y}$$

$$= -\delta_c\,[A \log(1 - \tilde{y}/\delta_c) + c_1(\tilde{x})\,\tilde{y}/\delta_c] \qquad (41)$$

The asymptotic behavior of $1 - \tilde{y}/\delta_c$ as $\tilde{\psi} \to \infty$ can be found from Eq. (41). Substitution in Eq. (40) and in $\tilde{p}/p_c = (\tilde{\rho}/\rho_c)^\gamma$ then gives

$$\tilde{p}/p_c \sim (A/A_c)^\gamma \exp\left[(A_c - A)\,(\gamma\tilde{\psi}/A A_c \delta_c)\right.$$

$$\left. - \gamma\,(c_{1,c}/A_c - c_1/A)\right]$$

where $c_{1,c} \equiv c_1(-\infty)$, $\rho_c \equiv \tilde{\rho}(-\infty, \tilde{y})$, and $p_c \equiv \tilde{p}(-\infty, \tilde{y}) = \hat{p}(0)$. If $\tilde{p}/p_c$ is to remain bounded and nonzero as $\tilde{\psi} \to \infty$,

$$A = c_0(\tilde{x}) + c_1(\tilde{x}) = \text{constant} \qquad (42)$$

$$\tilde{p}_\delta = p_c \exp\left[-\gamma A^{-1}(c_{1,c} - c_1)\right] \qquad (43)$$

where $\tilde{p}_\delta = \tilde{p}(\tilde{x}, \delta)$ and A is to be determined. Since $1/\tilde{\rho} = O(1 - \tilde{u})$, the velocity $\tilde{u}$ for $\tilde{y} \to \delta_c$ has the form $(1 - \tilde{u}) \sim$ (function of $\tilde{x}$) $\exp(-\tilde{\psi}/A\delta_c)$. It also follows from Eqs. (37), (40), and (42) that $\tilde{\rho}\tilde{v}$ and therefore $\tilde{\rho}\tilde{u}\tilde{v}$ are bounded and nonzero for $\tilde{u} \to 1$. The representation chosen for $\tilde{\rho}\tilde{u}\tilde{v}$ is

$$\tilde{\rho}\tilde{u}\tilde{v} = d_0(\tilde{x}) + d_1(\tilde{x})\,\tilde{y}/\delta_c \qquad (44)$$

The dependent variables for the one-strip calculation now include the four flow quantities $\tilde{u}$, $\tilde{v}$, $\tilde{p}$, and $\tilde{\rho}$ evaluated at $\tilde{y} = 0$ and the four coefficients c_0, c_1, d_0, and d_1. It is convenient to eliminate all the flow variables at $\tilde{y} = \delta_c$ except for $\tilde{p}$. Thus there are nine dependent variables. The available equations include the entropy and total enthalpy equations at $\tilde{y} = 0$; the boundary condition at $\tilde{y} = 0$; and the representations for $\tilde{\rho}\tilde{u}$ and $\tilde{\rho}\tilde{u}\tilde{v}$ evaluated at $\tilde{y} = 0$:

$$p_0 = [(\gamma - 1)/2\gamma]\,\rho_0^\gamma$$

$$u_0^2 + [2\gamma/(\gamma - 1)]\,p_0/\rho_0 = 1 \qquad (45)$$

$$v_o = 0 \ , \quad c_o = \rho_o u_o \ , \quad d_o = 0$$

where $u_o = \tilde{u}(\tilde{x}, 0)$, etc. At $\tilde{y} = \delta$ the condition $\tilde{v} = 0$ has been used to show that $\delta = \delta_c$ = constant, and the entropy and total enthalpy equations, combined with the representation of $\tilde{\rho}\,\tilde{u}$ for $\tilde{y} \to \delta_c$, have been used to obtain the relations (42) and (43). The remaining two of the necessary nine equations are the integrated continuity and $\tilde{y}$-momentum equations (37) and (38), specialized to the case N = 1. The representation for $\tilde{\rho}\,\tilde{u}\,\tilde{v}$ may be used to replace the right-hand side of the integrated continuity equation, and further simplification follows since $v_o = d_o = 0$:

$$c_1' = \delta_c^{-1} d_1 \qquad d_1' = -2\,\delta_c^{-1} (p_\delta - p_o) \qquad (46)$$

By combining these equations and replacing $\tilde{x}$ by the wall mach number M_o as the independent variable, one finds the pair of differential equations

$$d(d_1^2)/dM_o = 4\rho_o u_o (p_\delta - p_o) \times (1 - M_o^2) M_o^{-1} \left[1 + \tfrac{1}{2}(\gamma - 1) M_o^2\right]^{-1} \qquad (47)$$

$$d\tilde{x}/dM_o = \delta_c \rho_o u_o (1 - M_o^2) \times |d_1|^{-1} M_o^{-1} \left[1 + \tfrac{1}{2}(\gamma - 1) M_o^2\right]^{-1} \qquad (48)$$

The origin of coordinates is located by the condition $M_o(0) = 1$. Once a value of A has been chosen, the right-hand side of Eq. (47) depends only on M_o. The integration is started at the critical value $M_o = M_{o,c} = 0.448$, given in Eq. (36), and is continued until $M_o = 1$. Numerical results are discussed in Section 4.

The initial profile assumed for $\tilde{\rho}\,\tilde{u}$ can be shown to be consistent with the integral condition (1) for a critical point only for a single value of A. Expansions for $\Delta M_o \equiv M_o - M_{o,c} \to 0$ give

$$\tilde{p}_\delta - p_o \sim \gamma p_c M_{o,c} \left[1 + \tfrac{1}{2}(\gamma - 1) M_o^2\right]^{-1} \times \left[1 - A^{-1} \rho_{o,c} u_{o,c} (M_{o,c}^{-2} - 1)\right] \Delta M_o$$

$$\Delta\delta = \Delta \int_0^\infty (1/\tilde{\rho}\tilde{u})\, d\tilde{\psi} \sim (\Delta\tilde{p}_\delta / \gamma p_c) \int_0^{\delta_c} (\Delta\tilde{p}/\Delta\tilde{p}_\delta)(M_c^{-2} - 1)\, d\tilde{y}$$

It is required that $\Delta\delta = o(\Delta\tilde{p}_\delta)$. Since $M_c = M_c(\tilde{y})$ satisfies the integral condition (1), and since $\Delta\tilde{p}$ is expected to increase monotonically with $\tilde{y}$, it is necessary that $\Delta\tilde{p} - \Delta\tilde{p}_\delta = o(\Delta M_o)$ as $\Delta M_o \to 0$.

Thus the only consistent representation for $\tilde{\rho}\,\tilde{u}$, of the form assumed, has

$$A = \rho_{o,c} u_{o,c} (M_{o,c}^{-2} - 1) \qquad (49)$$

where $u_{o,c} = \tilde{u}(-\infty, 0)$, etc. The numerical value is A = 0.708. Since p_o and $\tilde{p}_\delta$ are known functions of M_o, the expansions for ΔM_o can be carried out to higher order to show that $\tilde{p}_\delta - p_o = O\{(M_o - M_{o,c})^2\}$. Since d_1 and $\bar{v}/\bar{u}$ are of the same order, it follows from Eq. (47) that $\bar{v}/\bar{u}_e = O\{(M_o - M_{o,c})^{3/2}\}$ as $M_o \to M_{o,c}$. This result is consistent with transonic small-disturbance theory; the flow deflection is of the same order as the perturbation in Mach number, or in pressure, raised to the three-halves power. Then Eqs. (44), (47), and (48) give $M_o - M_{o,c} = O(\tilde{x}^{-2})$ and $\tilde{v} = O(\tilde{x}^{-3})$ as $\tilde{x} \to -\infty$.

The numerical integration of Eqs. (47) and (48) makes use of initial conditions given in Eq. (21), which are based on the assumption that the zero-order solutions in terms of $\hat{x}$ and $\tilde{x}$ can be so matched. For higher-order approximations the situation would be quite different. As already noted, Eq. (34) gives $\bar{v}/\bar{u}_e = O(M_e^{-1}\,\hat{x}^{-1/2})$ as $\hat{x} \to 0$, but it has just been shown that $\bar{v}/\bar{u}_e = O(\tilde{x}^{-3})$ as $\tilde{x} \to \infty$. Thus these two representations of $\bar{v}/\bar{u}_e$ do not have the same functional form and the higher-order matching cannot be carried out. Since the expressions for $\bar{v}/\bar{u}_e$ are of the same order when $\tilde{x} = O(M_e^{1/5})$ it is expected that approximate equations must also be derived for the limit in which $\tilde{x}/M_e^{1/5}$ and $\tilde{y}$ are held fixed. In this limit the largest perturbations in the flow variables can be shown to be $\Delta\bar{u}/\bar{u}_e = O(M_e^{-2/5})$, $\Delta\bar{p}/\bar{\rho}_w\,\bar{u}_e^2 = O(M_e^{-2/5})$, $\Delta\bar{\rho}/\bar{\rho}_w = O(M_e^{-2/5})$, and $\bar{v}/\bar{u}_e = O(M_e^{-3/5})$. In a first approximation the governing equations in this limit include both the approximate momentum equation $\bar{p}_y \approx 0$ and the approximate boundary condition $\bar{v} \approx 0$ at $\bar{y} = \bar{\delta}$ *.

Since the coefficient d_1 approaches a nonzero constant as $\tilde{x} \to 0$, it follows from Eq. (48) that $1 - M_o = O(|\tilde{x}|^{1/2})$ as $\tilde{x} \to 0$. This behavior is also found by Gold and Holt[17] in a one-strip calculation by the method of integral relations for inviscid supersonic flow past a flat-faced cylinder. However, the similarity solution for irrotational transonic flow near a corner (for example, Fal'kovich and Chernov[18]), extended by Vaglio-Laurin[19] for rotational flow, would seem to suggest that the correct behavior is $1 - M_o = O(|\tilde{x}|^{2/5})$ as $\tilde{x} \to 0$. Apparently, integration across the layer relates the present problem to a one-dimensional flow

problem, because Eq. (48) has the same form (see Shapiro[20]) $dM^2/dx = G(x)/(1 - M^2)$ as would be obtained for a one-dimensional flow. In general, G(x) is required to be zero at M = 1, but if G(x) were to remain positive as $M \to 1$ the behavior would be the same as predicted above. It follows that the present theory cannot correctly predict details, such as the shape of the sonic line and the limiting characteristic, for $\tilde{x}^2 + \tilde{y}^2 \to 0$.

Integration of the sublayer equations (26) through (28), subject to the boundary and matching conditions (29), has been carried out using a one-strip method of integral relations. First new independent variables are introduced through the transformation[15]

$$\xi = \int_{-\infty}^{\tilde{x}} U(p^\dagger/p_e)\, d\tilde{x}\,, \quad \eta = U \int_0^{y^\dagger} \rho^\dagger\, dy^\dagger \qquad (50)$$

where $p_e = (\gamma - 1)/2\gamma$ and U is the composite solution (22) for $\bar{u}/\bar{u}_e$ evaluated at $\tilde{y} = 0$. Using

$$\frac{\partial}{\partial \tilde{x}} = \frac{d\xi}{d\tilde{x}} \left\{ \frac{\partial}{\partial \xi} - \frac{\partial \eta}{\partial y^\dagger} \int_0^\eta (1/\rho^\dagger U)_\xi\, d\eta\, \frac{\partial}{d\eta} \right\}$$

one finds the transformed equations

$$u_\xi^\dagger + w_\eta = 0 \qquad (51)$$

$$u^\dagger u_\xi^\dagger + w u_\eta^\dagger = (1 - u^{\dagger 2})\, M_o^{-1}\, dM_o/d\xi + u_{\eta\eta}^\dagger \qquad (52)$$

where M_o is the composite solution for the Mach number obtained in the manner of Eq. (22) and evaluated at $\tilde{y} = 0$, and

$$w = -\rho^\dagger U u^\dagger \int_0^\eta (1/\rho^\dagger U)_\xi\, d\eta + \rho^\dagger v^\dagger (p_e/p^\dagger)$$

A set of weighting functions $f_k(u^\dagger) = (1 - u^\dagger)^k$ is then introducted,[15] where k = 1, 2, . . . , N, and N will again be interpreted as the number of strips. Equations (51) and (52) are multiplied by f_k and f_k' respectively, and then added and integrated over η from 0 to ∞. Setting $\Theta = \partial \eta / \partial u^\dagger$, changing the variable of integration from η to $u^\dagger$, and integrating by parts, one finds

$$\frac{d}{d\xi} \int_0^1 f_k\, u^\dagger \Theta\, du^\dagger = \frac{1}{M_o} \frac{dM_o}{d\xi} \int_0^1 (1 - u^{\dagger 2})\, f_k' \Theta\, du^\dagger - \frac{f_k'(0)}{\Theta_o} - \int_0^1 \frac{f_k''}{\Theta}\, du^\dagger$$

where Θ_o is the value of Θ at $u^\dagger = 0$. If there were no pressure gradient, it would follow from the Blasius solution $g'(\beta)$ that $u_\eta^\dagger = O\{(1 - u^\dagger) \times [-\log (1 - u^\dagger)]^{1/2}\}$ as $u^\dagger \to 1$. The same behavior is assumed for a boundary layer with pressure gradient, and the behavior is again approximated by omitting the logarithmic factor. Thus Θ is represented by

$$\Theta = (1 - u^\dagger)^{-1} \sum_{m=0}^{N-1} a_m(\xi)\, u^{\dagger m}$$
$$\frac{1}{\Theta} = (1 - u^\dagger) \sum_{m=0}^{N-1} b_m(\xi)\, u^{\dagger m} \qquad (53)$$

where the coefficients a_m and b_m are related by the requirement that the representations for Θ and $1/\Theta$ be mutually consistent at strip boundaries $u_k = k/N$, where k = 0, 1, . . . , N-1. For N = 1 the differential equation and solutions are found to be

$$d\Theta_o^2/d\xi + 6 M_o^{-1} (dM_o/d\xi)\, \Theta_o^2 = 4$$

$$\Theta_o = 2 M_o^{-3} \left[\int_{-\infty}^{\xi} M_o^6\, d\xi \right]^{\frac{1}{2}}, \quad u^\dagger = 1 - e^{-\eta/\Theta_o} \qquad (54)$$

$$y^\dagger = \tfrac{1}{2} (\gamma - 1) \Theta_o (\gamma U p^\dagger)^{-1} \times \int_0^{u^\dagger} (1 - u^\dagger)^{-1} [1 - u^{\dagger 2} U^2]\, du^\dagger$$

$$\psi^\dagger = \Theta_o \int_0^{u^\dagger} (1 - u^\dagger)^{-1} u^\dagger du^\dagger$$

It follows from the definition of U and from the solutions already obtained that $U = O(\tilde{x}^{-1})$, and therefore $M_o = O(\tilde{x}^{-1})$, as $\tilde{x} \to -\infty$. Since the mass flow between the wall and any other streamline is constant, the value of $y^\dagger$ on any streamline must be $O(\tilde{x})$ as $\tilde{x} \to -\infty$. Integration from $\xi = -\infty$ in the result for Θ_o gives $\Theta_o = O(1)$ as $\tilde{x} \to -\infty$, and the solution for $y^\dagger$ therefore has the required behavior.

For $\tilde{x} \to -\infty$ one would expect that the velocity $\bar{u}/\bar{u}_e \sim U u^\dagger$ should match at the outer edge of the sublayer with the linear term $\bar{u}/\bar{u}_e = O(\tilde{y})$ of the Blasius profile and not with a velocity $U(\tilde{x})$. For $\tilde{x} \to -\infty$ along a streamline, $\tilde{y} = R_w^{-1/4} y^\dagger = O(R_w^{-1/4} \tilde{x})$ and $U = O(\tilde{x}^{-1})$ are of the same order when $\tilde{x} = O(R_w^{1/8})$, i.e., when $\bar{x}/L - 1 = O(R_w^{-3/8})$. This order estimate agrees with the estimate given by Lighthill[4] for the upstream influence of a weak

pressure disturbance in a supersonic boundary layer. The orders of all flow quantities for $\bar{x}/L - 1 = O(R_w^{-3/8})$ can be obtained by systematically studying the full equations, and it appears that the present results have the possibility of matching with a solution to the problem studied by Lighthill. While in the present work the perturbations in the flow quantities decay algebraically upstream as $\tilde{x} \to -\infty$, Lighthill predicts exponential decay as $R_w^{-1/8}\tilde{x} \to -\infty$.

4. DISCUSSION

Measurements of pressure near the base of a wedge have been obtained by Hama.[1] The largest free-stream Mach number considered corresponds to values $M_e = 4.02$, $R_w = 1.2 \times 10^4$, and $\bar{\delta}_1 = 0.10$ in., where $\bar{\delta}_1$ is the boundary-layer thickness just before the beginning of the expansion, found using the definition β following Eq. (8) and the total enthalpy equation:

$$R_w^{\frac{1}{2}}\,\bar{\delta}_1/L = 2^{\frac{1}{2}}\int_0^\infty \rho^{-1}\,d\beta$$

$$= 2^{\frac{1}{2}}\int_0^\infty (1 - g'^2)\,d\beta = 1.6864 \times 2^{\frac{1}{2}}$$

Although even this value of M_e might be rather low for use of a hypersonic theory, the other sources of error to be considered seem to be at least as important. In Fig. 4 of Ref. 7 the ratio $\bar{p}_o/\bar{p}_{e,i}$ is plotted against $\bar{x}$ for three different Mach numbers, where $\bar{p}_o$ is the measured surface pressure from Ref. 1 and $\bar{p}_{e,i}$ is the surface pressure predicted by inviscid-flow theory. In the experiments the static pressure orifice furthest upstream from the corner was located at a distance $\bar{x} - L = -1.5$ in., where $L = 4.783$ in., and it is pointed out in Ref. 7 that $\bar{p}_o$ at this location is larger than $\bar{p}_{e,i}$ because of viscous interaction. The data shown in Ref. 7 are replotted here as Fig. 3, using values taken partly from data supplied by Hama and partly from the figure of Ref. 7. The same data are plotted in Fig. 4 in the form $\bar{p}_o/\bar{p}_e$ vs $\tilde{x}/\delta_1 \equiv (\bar{x} - L)/\bar{\delta}_1$, where $\delta_1 \equiv R_w^{1/2}\,\bar{\delta}_1/L$ and $\bar{p}_e$ is the measured pressure at the orifice furthest upstream. It can be seen from Fig. 4 that the wall pressure ratio measurements plotted in this way are nearly independent of the Reynolds number R_w, as would be predicted by the theory.

Also shown in Fig. 4 are the pressure ratio solution $\hat{p}(\hat{x})$ plotted against $\tilde{x} = M_e\hat{x}$ for $M_e = 4.02$, the solution $\tilde{p}(\tilde{x}, 0)$, and the corresponding composite solution (22). Each has been multiplied by $\bar{\rho}_w\bar{u}_e^2/\bar{p}_e$, so that the values plotted are values of $\bar{p}_o/\bar{p}_e$. The discrepancy between the calculated composite solution and the experimental data is seen to be $|\Delta\bar{p}/\bar{p}| \approx 0.06$ or less. This might be regarded as a rather good result, as compared with the accuracy usually obtained in a one-strip calculation by the method of integral relations. However, the apparent accuracy probably occurs partly because the result found by the method of integral relations comprises only part of the solution, the first part of the pressure drop having been obtained analytically.

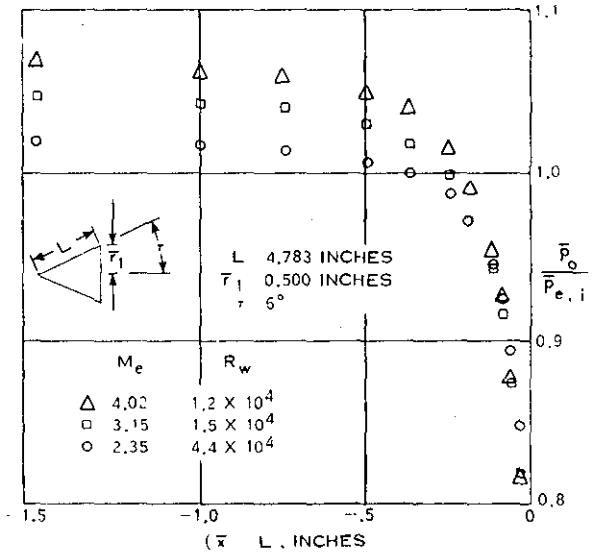

Figure 3. Hama's Wall Pressure Data for Laminar Flow

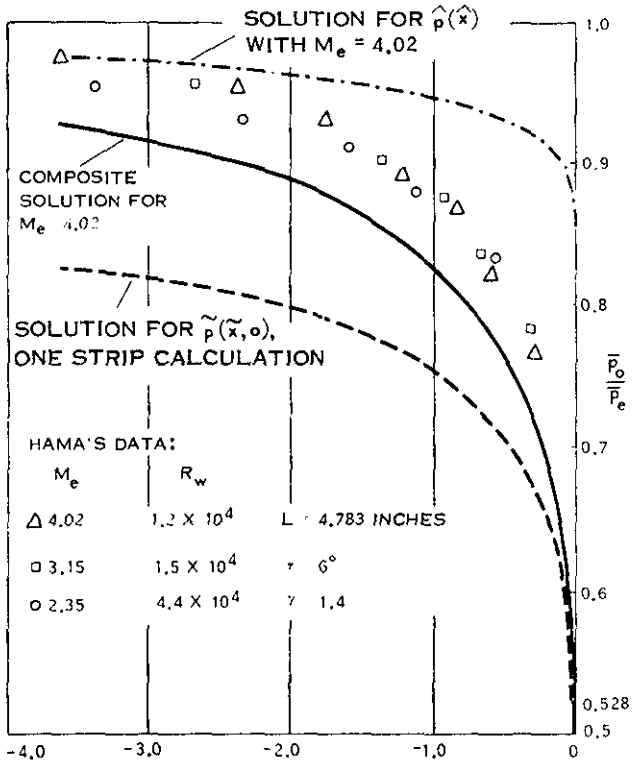

Figure 4. Comparison of Composite Solution for the Wall Pressure-Ratio with Hama's Data

The magnitude of the interaction effect upstream of the corner expansion, as shown by Fig. 3, perhaps should suggest the importance of the analogous displacement effect of the sublayer. The sublayer displacement thickness is positive because fluid in the sublayer is retarded relative to fluid in the main part of the boundary layer, but is decreasing because each fluid element in the sublayer undergoes a small positive acceleration and consequently the streamlines are deflected slightly toward the wall. As explained in Sections 2 and 3, the flow deflection and the pressure perturbation in the sublayer are $O(R_w^{-1/4})$. The resulting perturbations in the main part of the boundary layer are also $O(R_w^{-1/4})$ and may be described by inviscid-flow equations because neglected viscous forces are $O(R_w^{-1/2})$, the same order as the perturbations due to ordinary viscous interaction further upstream. If terms $O(R_w^{-1/4})$ are included, the pressure at the corner is still the sonic value, and so the overall pressure drop is unchanged. Thus the major effect of the sublayer is to change slightly the effective shape of the surface, thereby steepening the pressure drop close to the corner and shifting the middle part of the pressure curve in Fig. 4 slightly downstream. This predicted shift would lead to better agreement with experimental results. A second correction of the same order arises through the upstream behavior discussed at the end of Section 3. If for simplicity the Mach number is again held fixed it appears that a solution is needed for $\bar{x}/L - 1 = O(R_w^{-3/4})$ in order to complete the higher order upstream matching. Since the pressure perturbation in the present solutions has been found to decay as $R_w^{-1}(\bar{x}/L - 1)^{-2}$, it is expected that in this limit $(\bar{p} - \bar{p}_e)/\bar{p}_e = O(R_w^{-1/4})$. That is, a pressure drop of this order would begin at a larger distance upstream than is shown in Fig. 4, and the upstream part of the composite pressure curve would be shifted slightly downward. One might guess that this effect is important primarily at large values of $|\tilde{x}|$ and that the sublayer effect is more important at small and moderate values of $|\tilde{x}|$.

According to the theory, the pressure drop plotted in Fig. 4 should begin further upstream at higher Mach numbers, because the proper nondimensional coordinate is $\hat{x} = M_e^{-1}\,\tilde{x}$ for the initial part of the expansion. It is evident that the data in Fig. 4 do not show this behavior. For the given values of M_e and R_w the sublayer effect would oppose the predicted effect of Mach number. If the sublayer effect were the major source of error, the predicted behavior with Mach number might well be obscured.

Other errors would result from neglecting higher-order terms in Mach number. The first step toward studying Mach number corrections would be to consider the special limit for $\tilde{x}/M_e^{1/3}$ held fixed, as noted in Section 3, but it seems impossible to guess the qualitative nature of the correction that would be found. Another Mach number effect arises because in the hypersonic approximation $\bar{T}/\bar{T}_w = 0$ at $\tilde{y} = \delta$, whereas actually $\bar{T}/\bar{T}_w$ should decrease smoothly from $O(1)$ to $O(M_e^{-2})$. In principle the nonuniformity might be removed by developing a theory analogous to that of Bush[21] for a very thin region near $\tilde{y} = \delta$.

The changes in velocity profile for the accelerating boundary layer are shown in Fig. 5 by plots of $\bar{u}/\bar{u}_e$ vs. $\tilde{\psi}$. The two solid curves represent the initial velocity profile $\bar{u}/\bar{u}_e = \hat{u}(-\infty, \tilde{y}) = g'(\beta)$ and the profile $\bar{u}/\bar{u}_e = \hat{u}(0, y)$ given by the upstream solution (33) at $\hat{x} = 0$. It is evident that the initial acceleration of fluid particles along streamlines is significant only near the wall, but plots of $\bar{u}/\bar{u}_e$ vs. $\tilde{y}$ would show that the resulting displacement of streamlines is significant all across the layer. For the solution in terms of $\tilde{x}$ and $\tilde{y}$, it is probably consistent with a one-strip calculation by the method of integral relations to choose only a linear variation of $\tilde{u}$ with $\tilde{y}$:

$$\tilde{u} = u_o + (1 - u_o)\,\tilde{y}/\delta_c \qquad (55)$$

Eqs. (55) and (41) can be combined to give plots of $\bar{u}/\bar{u}_e$ vs. $\tilde{\psi}$ for $\tilde{x} \to -\infty$ and $\tilde{x} = 0$, shown as dotted curves in Fig. 5. Good agreement is obtained between the approximate form for $\tilde{u}$ as $\tilde{x} \to -\infty$ and the solution (33) for $\hat{u}$ at $\hat{x} = 0$. Although the profile $\bar{u}/\bar{u}_e$ at the corner $\tilde{x} = 0$ may also be fairly accurate, the behavior of derivatives with respect to $\tilde{x}$ is not given correctly as $\tilde{x} \to 0$ because the singularity at the corner is not properly taken into account by the integral method. Therefore it is not clear how the present procedure might be used to obtain a profile for the flow deflection at $\tilde{x} = 0$.

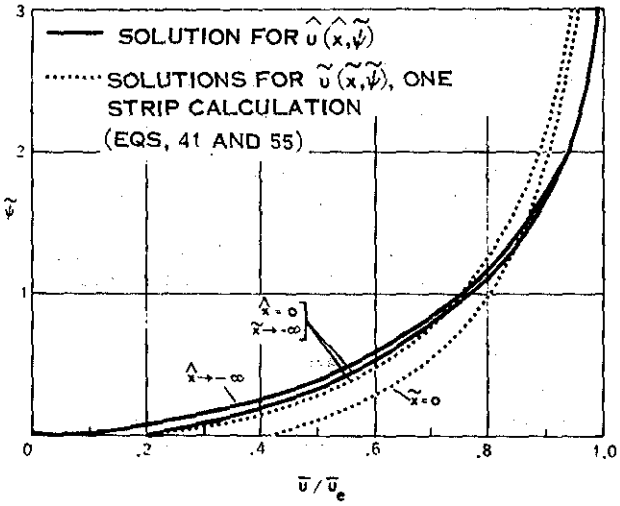

Figure 5. Velocity Profile at Three Stations: $\hat{x} \to -\infty$, $\hat{x} = 0$ ($\tilde{x} \to -\infty$), and $\tilde{x} = 0$

In an attempt to improve the accuracy of the numerical method, a two-strip calculation was investigated in which the intermediate strip boundary was taken to be the streamline at which the fluid velocity was initially sonic. This formulation is described in Ref. 16. In addition to complications in the derivation of upstream asymptotic expansions for $\tilde{x} \to -\infty$, there was a conceptual difficulty because it was not evident how the procedure would be extended for a third strip boundary with initially subsonic fluid velocity. There appears in one of the differential equations a denominator which would vanish at a point where $\bar{u} = a^*$, the critical sound speed, exactly as in the application of the method of integral relations to problems of inviscid flow past flat-faced bodies." The solution should pass smoothly through this point, and so the corresponding numerator is required to vanish simultaneously. In the formulation described in Ref. 16 the initial conditions and expansions for $\tilde{x} \to -\infty$ appeared to determine the solution completely, and so no downstream condition could be imposed. As long as this situation is not understood, the calculation for a strip boundary initially sonic would also be suspect.

In order to significantly improve the accuracy, it would be necessary to improve the numerical procedure and to derive some or all of the higher-order corrections described. It seems especially desirable to consider higher-order viscous effects in greater detail. Although insufficient data are available for a thorough check against experimental results, the present solutions are expected to be at least qualitatively correct, and require only a rather simple numerical procedure. The assumption of a small interaction parameter $M_e R_w^{-1/2}$ was essential in limiting the viscous effects near the corner to a thin sublayer, and cannot be relaxed in this analysis. Use of the hypersonic approximation permits the Mach number M_e effectively to be removed from the problem, since the analytical and numerical parts of the solution can be obtained without specifying M_e, and shows rather clearly the significance of the critical point.

REFERENCES

1. Hama, F.R., "Experimental Investigations of Wedge Base Pressure and Lip Shock," Calif. Inst. of Tech. Jet Propulsion Lab., Tech. Rep. No. 32-1033 (1966).

2. Moore, F.K., "Hypersonic Boundary Layer Theory," Theory of Laminar Flows, ed. F.K. Moore (Princeton Univ. Press, Princeton, 1964), pp. 491-492.

3. Morkovin, M.V., "Effects of High Acceleration on a Turbulent Supersonic Shear Layer," Proc. of 1955 Heat Trans. and Fluid Mech. Inst. (Stanford Univ. Press, Stanford, Calif., 1955).

4. Lighthill, M.J., "On Boundary Layers and Upstream Influence. II. Supersonic Flows without Separation," Proc. Roy. Soc. A 217, 478-507 (1953).

5. Zakkay, V. and Tani, T., "Theoretical and Experimental Investigation of the Laminar Heat Transfer Downstream of a Sharp Corner," Polytechnic Institute of Brooklyn, Dept. of Aerospace Eng. and Appl. Mech., PIBAL Rept. No. 708 (1961).

6. Hunt, B.L. and Sibulkin, M., "An Estimate of Compressible Boundary Layer Development Around a Convex Corner in Supersonic Flow," Brown University, Div. of Engineering, Rept. No. Nonr (562)35/6 (1964).

7. Baum, E., "An Interaction Model of a Supersonic Laminar Boundary Layer Near a Sharp Backward Facing Step," TRW Systems, BSD TR 67-81 (1966).

8. Weiss, R.F. and Nelson, W., "On the Upstream Influence of the Base Pressure," AVCO Everett Research Report 264 (1967).

9. Lees, L. and Reeves, B.L., "Supersonic Separated and Reattaching Laminar Flows: I. General Theory and Application to Adiabatic Shock-Wave/Boundary-Layer Interactions," AIAA J. 2, 1907-1924 (1964).

10. Lees, L., "Fluid Mechanics of Wakes," presented at AGARD Conference on Fluid Physics of Hypersonic Wakes, Colorado State Univ., Fort Collins, Colo., (1967).

11. Cole, J.D. and Aroesty, J., "The Blowhard Problem - Inviscid Flows with Surface Injection," RAND Corp., Memorandum RM-5196-ARPA (1967).

12. Liepmann, H. and Roshko, A., Elements of Gasdynamics (Wiley, New York, 1957), p. 268

13. Kaplun, S., Fluid Mechanics and Singular Perturbations, ed. P.A. Lagerstrom, L. N. Howard, and C. S. Liu (Academic Press, New York, 1967).

14. Rosenhead, L. (ed), Laminar Boundary Layers (Oxford Univ. Press, Oxford, England, 1963) p. 224.

15. Belotserkovskii, O.M. and Chushkin, P. I., "The Numerical Solution of Problems in Gas Dynamics," Basic Developments in Fluid Dynamics, ed. M. Holt (Academic Press, New York, 1965), pp. 1-126.

16. Olsson, G.R. and Messiter, A.F., "Acceleration of a Hypersonic Boundary Layer Approaching a Corner," Willow Run Laboratories of the Institute of Science and Technology, Univ. of Michigan, Rept. No. 8416-13-T (1967).

17. Gold, R. and Holt, M., "Calculation of Supersonic Flow Past a Flat-Headed Cylinder by Belotserkovskii's Method," Brown Univ., Div. of Appl. Math., AFOSR Tech. Note No. 59-199 (1959).

18. Fal'kovich, S.V. and Chernov, I.A., "Flow of a Sonic Gas Stream Past a Body of Revolution," PMM 28, 280-284 (1964); Transl.: J. Appl. Math. and Mech. 28, 342-347 (1964).

19. Vaglio-Laurin, R., "Transonic Rotational Flow over a Corner," J. Fluid Mech. 9, 81-103 (1960).

20. Shapiro, A.H., The Dynamics and Thermodynamics of Compressible Fluid Flow (Ronald Press, New York, 1953), Vol. I, pp. 255-260.

21. Bush, W.B., "Hypersonic Strong-Interaction Similarity Solutions for Flow Past a Flat Plate," J. Fluid Mech. 25, 51-64 (1966).